Surface electric current distributions on spheres and spheroids as sources of pure quadrupole magnetic fields

L. Medina
Facultad de Ciencias, Universidad Nacional Autónoma de México.

E. Ley-Koo
Instituto de Física, Universidad Nacional Autónoma de México,
Apartado Postal 20-364, México, D.F., 01000, México.

Recibido el 24 de enero de 2011; aceptado el 3 de mayo de 2011

Neutral atom magnetic traps and nuclear magnetic resonance imaging require internal regions with constant gradient magnetic induction fields, which are identified as pure quadrupole fields. This contribution starts from such fields in the interior of spheres and spheroids in cartesian coordinates, identifying immediately their respective scalar magnetic potentials. Next, the corresponding potentials inside and outside are constructed using spherical and spheroidal harmonic functions, respectively, except for a proportionality constant to be determined by the boundary conditions at the surface of spheres $r = a$, prolate $\xi = \xi_0$ and oblate $\zeta = \zeta_0$ spheroids, where the electric current sources are distributed. The negative gradients of the scalar potentials yield the respective magnetic induction fields inside ($r \leq a$, $\xi \leq \xi_0$, $\zeta \leq \zeta_0$) and outside ($r \geq a$, $\xi \geq \xi_0$, $\zeta \geq \zeta_0$). Gauss's law in its boundary condition form determines the normalization constant of the external potentials, while Ampere's law determines the electric current source distributions on the surface of the spheres and spheroids.

Keywords: Quadrupole magnetic fields and surface sources; constant gradient magnetic field; gradient coil windings; spherical and spheroidal harmonics.

Trampas de átomos neutros e imageneología por resonancia magnética requieren de regiones internas con campos de inducción magnética de gradiente constante. Esta contribución parte de tales campos en el interior de esferas y esferoides en coordenadas cartesianas, identificando inmediatamente sus respectivos potenciales magnéticos escalares. A continuación, los potenciales interiores y exteriores correspondientes se construyen usando funciones armónicas esféricas y esferoidales, respectivamente, excepto por una constante de proporcionalidad por determinarse vía las condiciones de frontera sobre la superficie de esferas $r = a$, esferoides prolatos $\xi = \xi_0$ y oblatos $\zeta = \zeta_0$, donde las fuentes de corriente eléctricas se distribuyen. Los negativos de los gradientes de los potenciales escalares conducen a los campos de inducción magnética respectivos en el interior ($r \leq a$, $\xi \leq \xi_0$, $\zeta \leq \zeta_0$) y en el exterior ($r \geq a$, $\xi \geq \xi_0$, $\zeta \geq \zeta_0$). La ley de Gauss en su forma de condición de frontera determina la constante de normalización para los potenciales externos, mientras que la ley de Ampère determina las distribuciones de corriente eléctrica sobre la superficie de las esferas y esferoides.

Descriptores: Campos magnéticos y fuentes superficiales cuadrupolares; campos magnético de gradiente constante; embobinados de gradiente; armónicos esféricos y esferoidales.

PACS: 41.20.Gz

1. Introduction

The question "Which coil windings with electric currents and on which surfaces will produce constant gradient magnetic fields?" formulates the problem of interest in this article. An exact answer is expressed in the proper magnetostatic mathematical language in its Title; with a summary of the hypothesis and method for the quantitative construction of its answer in the Abstract; a detailed analysis of the successive steps in the respective sections of the article, including the illustrative graphic results of Fig. 1 for the coil windings on a sequence of prolate spheroids, spheres and oblate spheroids, producing pure quadrupole fields inside and outside; an Appendix leading the reader from the coordinate transformations to the needed spheroidal harmonic funtions; and a discussion of the contents with didactic observations.

The problem itself has been of interest in different fields of basic science and of its applications. Here the illustration is restricted to its relevance in neutral atom traps [1] and nuclear magnetic resonance imaging [2]. In fact, Ref. 1 with the title "Magnetostatic traps for charged and neutral particles" analyzes the dynamics of cold neutral atoms and their loss mechanisms in a quadrupole magnetostatic trap. The complementary use of three pairs of converging and mutually orthogonal laser beams in a magneto-optic trap, MOT, was behind the investigations of Chu, Cohen-Tannoudji and Williams recognized by the Nobel Prize in Physics 1997 [3] "for development of methods to cool and trap atoms with laser light", and of Cornell, Ketterle and Wieman who shared the same prize in 2001 [4] "for the achievement of Bose-Einstein condensation in dilute gases of alkali atoms and for early fundamental studies of the properties of the condensates". Related advances in other fields of physics include lowering the achievable and measurable temperatures from microkelvins to nanokelvins, producing atom interferometry, and atom lasers. By the same token, the Nobel Prize in Physiology or Medicine 2003 [5] was awarded to Lauterbur and Mansfield for their discoveries concerning "magnetic resonance imaging". Specifically, in the early 1970's Lauterbur discovered the possibility to create a two-dimensional picture by introducing constant gradients in the magnetic field; and

Mansfield discovered that the use of such gradients gave signals that rapidly and effectively could be analyzed and transformed to an image, and he also showed how extremely rapid imaging could be achieved by very fast gradient variations. By 2003 more that 60 million investigations with MRI per year were performed worldwide. Reference 2, with the title "Theory of Gradient Coil Design Methods for Magnetic Resonance Imaging", focuses on the importance of constant gradient magnetic fields as the necessary condition to perform space localization of the magnetic resonance signals. It is a very recent review on the methods to design gradient coils developed in the last two decades; some of its references illustrating the latest methods of design for cylindrical [6], hemispherical [7-8], planar [9-10], and open geometries [11] are cited as points of comparison. It also recognizes that the search for the optimum coil windings is still an open one.

The reader is advised that this is a teaching article in magnetostatics providing an answer to the opening question in this section. The answer for spheres is implicit in an earlier teaching article "The multipole expansion outside and inside", covering the electrostatic and magnetostatic situations -inlcuding magnetic vector and scalar potentials- and giving examples of traps for charged particles and for neutral particles with a magnetic dipole moment [12]. The general theorem: 2^ℓ- multipole fields inside and outside a sphere are produced by 2^ℓ- multipole sources on the surface of the sphere, applied to the special case of ℓ=2, gives the explicit answer for the quadrupole magnetic fields and sources in a sphere. Next, the answers for the prolate and oblate spheroids are constructed step by step.

The quadrupole nature of the magnetic field is based on the following reasoning. Since it is a constant gradient field, it must be a linear function in the x,y,z coordinates. Consequently, it is derivable from a quadratic potential in the same coordinates with ℓ=2. The potential may be chosen at will as a scalar potential or a vector potential [12-15]. In fact, inside and outside the spheroids the magnetic induction field is solenoidal and irrotational, allowing it to be expressed in the alternative forms $B^R = \nabla \times \vec{A}^R$ or $\vec{B}^R = -\nabla\phi^R$ for $R = i, e$ the internal and external regions, respectively. Both potentials statisfy the Laplace equation and therefore must be harmonic functions, with multipolarity ℓ=2 in the specific case under discussion. Here we choose the scalar potential because its use is familiar to most readers.

In this article, we take as the starting point the following target constant gradient magnetic induction fields, with a gradient parameter *G*, in the interior of spheres and spheroids:

$$\vec{B}^i(\vec{r}) = G\left(-\hat{i}x - \hat{j}y + 2\hat{k}z\right), \tag{1.1}$$

$$\vec{B}^i(\vec{r}) = G\left(\hat{i}z + \hat{k}x\right), \tag{1.2}$$

$$\vec{B}^i(\vec{r}) = G\left(\hat{j}z + \hat{k}y\right), \tag{1.3}$$

$$\vec{B}^i(\vec{r}) = G\left(-\hat{i}x + \hat{j}y\right), \tag{1.4}$$

$$\vec{B}^i(\vec{r}) = G\left(\hat{i}y + \hat{j}x\right). \tag{1.5}$$

The reader may easily ascertain that they are solenoidal $\nabla \cdot \vec{B} = 0$, curl-less $\nabla \times \vec{B} = 0$, and consequently harmonic $\nabla^2\vec{B} = 0$ [12-15].

The problem of our interest is to evaluate the electric current distributions or coil windings, on the surfaces of spheres $r = a$, prolate $\xi = \xi_0$ and oblate $\zeta = \zeta_0$ spheroids, that may generate the magnetic induction fields in Eqs. (1.1-1.5).

The first step is to recognize that the following scalar magnetic potentials:

$$\phi^i(\vec{r}) = \frac{1}{2}G\left(x^2 + y^2 - 2z^2\right), \tag{1.6}$$

$$\phi^i(\vec{r}) = -Gxz, \tag{1.7}$$

$$\phi^i(\vec{r}) = -Gyz, \tag{1.8}$$

$$\phi^i(\vec{r}) = \frac{1}{2}G\left(x^2 - y^2\right), \tag{1.9}$$

$$\phi^i(\vec{r}) = -Gxy. \tag{1.10}$$

lead to the respective magnetic induction fields of Eqs. (1.1-1.5) via $\vec{B} = -\nabla\phi$. The reader may also establish the harmonic character of the potentials by evaluating $\nabla^2\phi = 0$, and that their degree ℓ=2 determines its quadrupole character.

In Sec. 2, the internal magnetic potentials of Eqs. (1.6-1.10) are rewritten in terms of spherical and spheroidal harmonic functions with ℓ=2, *i.e.* quadrupole harmonics, with m=0, 1, 2 involving $\cos(m\varphi)$ and $\sin(m\varphi)$ functions with well-defined parities. The Appendix contains the transformation equations among cartesian, prolate and oblate spheroidal coordinates; their scale factors and unit vectors; the Laplace operator, the Laplace equation, and its solutions in the respective coordinates. The scalar magnetic potentials outside the spheroids are constructed from the inside ones with the replacements of Legendre polynomials by Legendre functions of the second kind, regular at infinity, $P_m^\ell(\xi) \to Q_m^\ell(\xi)$ and $P_m^\ell(i\zeta) \to Q_m^\ell(i\zeta)$, respectively, and a proportionality factor to be determined by the continuity of the normal derivatives at the surface of the spheroids $\xi = \xi_0$ and $\zeta = \zeta_0$. In the case of spheres the corresponding radial factors are $r^2/a^3 \to a^2/r^3$ [12].

In Sec. 3, the evaluation of the negative gradient of the potentials yields the respective magnetic induction fields inside and outside the spheres and spheroids. Gauss's law in its boundary condition form requires that the normal components are continuous $\hat{n} \cdot \left(\vec{B^e} - \vec{B^i}\right) = 0$ at $r = a$, $\xi = \xi_0$ and $\zeta = \zeta_0$, corresponding to the non existence of magnetic charges. On the other hand, Ampere's law connects the discontinuities in the tangential components with the surface electric current distribution, $\hat{n} \times \left(\vec{B^e} - \vec{B^i}\right) = 4\pi\vec{K}/c$ in Sec. 4. The field lines for the electric current per unit length $\vec{K}$ on the spheres and spheroids are also evaluated in

Sec. 4, and displayed graphically and discussed in Sec. 5; some didactic observations and additional references are also included in the last section.

2. Scalar magnetic potentials inside and outside

The scalar magnetic potentials in Eqs. (1.6-1.10) and the quadrupole spheroidal harmonic functions of Eqs. (A.18-A.23) are recognized to have the same space dependencies when the transformation Eqs. (A.1) are used. Here we rewrite them in the general compact forms:

$$\begin{aligned}
\phi_2^m\left(r<a,\vartheta,\varphi\right) &= B_0^i \frac{r^2}{a} P_2^m\left(\cos\vartheta\right) \\
&\quad \times \begin{pmatrix} \cos\left(m\varphi\right) \\ \sin\left(m\varphi\right) \end{pmatrix}, \\
\phi_2^m\left(\xi<\xi_0,\vartheta,\varphi\right) &= B_0^i f P_2^m\left(\xi\right) P_2^m\left(\cos\vartheta\right) \\
&\quad \times \begin{pmatrix} \cos\left(m\varphi\right) \\ \sin\left(m\varphi\right) \end{pmatrix}, \\
\phi_2^m\left(\zeta<\zeta_0,\vartheta,\varphi\right) &= B_0^i f P_2^m\left(i\zeta\right) P_2^m\left(\cos\vartheta\right) \\
&\quad \times \begin{pmatrix} \cos\left(m\varphi\right) \\ \sin\left(m\varphi\right) \end{pmatrix},
\end{aligned} \tag{2.1}$$

in the spherical, prolate and oblate spheroidal coordinates for the interior of the respective spheres and spheroids, $r = a$, $\xi = \xi_0$ and $\zeta = \zeta_0$. Instead of the *G* coefficient in Eqs. (1.1-1.10) as a measure of the constant gradient of the magnetic induction fields, we introduce the B_0^i coefficient as a measure of the strength of the field itself. From here on both functions $\cos\left(m\varphi\right)$ and $\sin\left(m\varphi\right)$ are treated at the same time and on the same footing.

The companion potentials for the exterior are written next by using an appropriate B_0^e strength coefficient, and the replacements $r^2/a^3 \to a^2/r^3$ [12], $P_2^m\left(\xi\right) \to Q_2^m\left(\xi\right)$, and $P_2^m\left(i\zeta\right) \to Q_2^m\left(i\zeta\right)$, Eqs. (A.24), guaranteeing that the potentials vanish for $r \to \infty$, $\xi \to \infty$, and $\zeta \to \infty$:

$$\begin{aligned}
\phi_2^m\left(r\geq a,\vartheta,\varphi\right) &= B_0^e \frac{a^4}{r^3} P_2^m\left(\cos\vartheta\right) \\
&\quad \times \begin{pmatrix} \cos\left(m\varphi\right) \\ \sin\left(m\varphi\right) \end{pmatrix}, \\
\phi_2^m\left(\xi\geq\xi_0,\vartheta,\varphi\right) &= B_0^e f Q_2^m\left(\xi\right) P_2^m\left(\cos\vartheta\right) \\
&\quad \times \begin{pmatrix} \cos\left(m\varphi\right) \\ \sin\left(m\varphi\right) \end{pmatrix}, \\
\phi_2^m\left(\zeta\geq\zeta_0,\vartheta,\varphi\right) &= B_0^e f Q_2^m\left(i\zeta\right) P_2^m\left(\cos\vartheta\right) \\
&\quad \times \begin{pmatrix} \cos\left(m\varphi\right) \\ \sin\left(m\varphi\right) \end{pmatrix}.
\end{aligned} \tag{2.2}$$

3. The magnetic induction fields inside and outside: continuity of their normal components at the surfaces

The magnetic induction fields inside and outside the spheres and spheroids are evaluated as the negative gradients of the respective potentials in Eqs. (2.1) and (2.2):

$$\vec{B}\left(r\leq a,\vartheta,\varphi\right) = -\frac{B_0^i}{a}\left[\left(\hat{r}2rP_2^m\left(\cos\vartheta\right)+\hat{\vartheta}r\frac{dP_2^m\left(\cos\vartheta\right)}{d\vartheta}\right)\begin{pmatrix}\cos\left(m\varphi\right)\\ \sin\left(m\varphi\right)\end{pmatrix}+\hat{\varphi}\frac{rm}{\sin\vartheta}P_2^m\left(\cos\vartheta\right)\begin{pmatrix}-\sin\left(m\varphi\right)\\ \cos\left(m\varphi\right)\end{pmatrix}\right], \tag{3.1}$$

$$\vec{B}\left(r\geq a,\vartheta,\varphi\right) = -\frac{B_0^e a^4}{r^4}\left[\left(-\hat{r}3P_2^m\left(\cos\vartheta\right)+\hat{\vartheta}\frac{dP_2^m\left(\cos\vartheta\right)}{d\vartheta}\right)\begin{pmatrix}\cos\left(m\varphi\right)\\ \sin\left(m\varphi\right)\end{pmatrix}+\hat{\varphi}\frac{m}{\sin\vartheta}P_2^m\left(\cos\vartheta\right)\begin{pmatrix}-\sin\left(m\varphi\right)\\ \cos\left(m\varphi\right)\end{pmatrix}\right], \tag{3.2}$$

$$\begin{aligned}
\vec{B}\left(\xi\leq\xi_0,\vartheta,\varphi\right) = -B_0^i f\Bigg[&\left(\frac{\hat{\xi}}{h_\xi}\frac{dP_2^m\left(\xi\right)}{d\xi}P_2^m\left(\cos\vartheta\right)+\frac{\hat{\vartheta}}{h_\vartheta}P_2^m\left(\xi\right)\frac{dP_2^m\left(\cos\vartheta\right)}{d\vartheta}\right)\begin{pmatrix}\cos\left(m\varphi\right)\\ \sin\left(m\varphi\right)\end{pmatrix} \\
&+\hat{\varphi}\frac{m}{h_\varphi}P_2^m\left(\xi\right)P_2^m\left(\cos\vartheta\right)\begin{pmatrix}-\sin\left(m\varphi\right)\\ \cos\left(m\varphi\right)\end{pmatrix}\Bigg],
\end{aligned} \tag{3.3}$$

$$\begin{aligned}
\vec{B}\left(\xi\geq\xi_0,\vartheta,\varphi\right) = -B_0^e f\Bigg[&\left(\frac{\hat{\xi}}{h_\xi}\frac{dQ_2^m\left(\xi\right)}{d\xi}P_2^m\left(\cos\vartheta\right)+\frac{\hat{\vartheta}}{h_\vartheta}Q_2^m\left(\xi\right)\frac{dP_2^m\left(\cos\vartheta\right)}{d\vartheta}\right)\begin{pmatrix}\cos\left(m\varphi\right)\\ \sin\left(m\varphi\right)\end{pmatrix} \\
&+\hat{\varphi}\frac{m}{h_\varphi}Q_2^m\left(\xi\right)P_2^m\left(\cos\vartheta\right)\begin{pmatrix}-\sin\left(m\varphi\right)\\ \cos\left(m\varphi\right)\end{pmatrix}\Bigg],
\end{aligned} \tag{3.4}$$

$$\begin{aligned}
\vec{B}\left(\zeta\leq\zeta_0,\vartheta,\varphi\right) = -B_0^i f\Bigg[&\left(\frac{\hat{\zeta}}{h_\zeta}\frac{dP_2^m\left(i\zeta\right)}{d\zeta}P_2^m\left(\cos\vartheta\right)+\frac{\hat{\vartheta}}{h_\vartheta}P_2^m\left(i\zeta\right)\frac{dP_2^m\left(\cos\vartheta\right)}{d\vartheta}\right)\begin{pmatrix}\cos\left(m\varphi\right)\\ \sin\left(m\varphi\right)\end{pmatrix} \\
&+\hat{\varphi}\frac{m}{h_\varphi}P_2^m\left(i\zeta\right)P_2^m\left(\cos\vartheta\right)\begin{pmatrix}-\sin\left(m\varphi\right)\\ \cos\left(m\varphi\right)\end{pmatrix}\Bigg],
\end{aligned} \tag{3.5}$$

$$\vec{B}\left(\zeta \geq \zeta_0, \vartheta, \varphi\right) = -B_0^e f \left[\left(\frac{\hat{\zeta}}{h_\zeta} \frac{dQ_2^m\left(i\zeta\right)}{d\zeta} P_2^m\left(\cos\vartheta\right) + \frac{\hat{\vartheta}}{h_\vartheta} Q_2^m\left(i\zeta\right) \frac{dP_2^m\left(\cos\vartheta\right)}{d\vartheta} \right) \begin{pmatrix} \cos\left(m\varphi\right) \\ \sin\left(m\varphi\right) \end{pmatrix} + \hat{\varphi} \frac{m}{h_\varphi} Q_2^m\left(i\zeta\right) P_2^m\left(\cos\vartheta\right) \begin{pmatrix} -\sin\left(m\varphi\right) \\ \cos\left(m\varphi\right) \end{pmatrix} \right]. \quad (3.6)$$

Gauss's law requires that the normal components of the magnetic induction field at the surfaces $r = a$, $\xi = \xi_0$ and $\zeta = \zeta_0$ are continuous, which determine the relationships between the coefficients B_0^e and B_0^i:

$$-3B_0^e = 2B_0^i, \quad (3.7)$$

$$B_0^e \frac{dQ_2^m\left(\xi\right)}{d\xi} \mid_{\xi=\xi_0} = B_0^i \frac{dP_2^m\left(\xi\right)}{d\xi} \mid_{\xi=\xi_0}, \quad (3.8)$$

$$B_0^e \frac{dQ_2^m\left(i\zeta\right)}{d\zeta} \mid_{\zeta=\zeta_0} = B_0^i \frac{dP_2^m\left(i\zeta\right)}{d\zeta} \mid_{\zeta=\zeta_0}. \quad (3.9)$$

4. Discontinuities of the tangential components of the magnetic induction fields at the surfaces leading to the distribution of the surface electric current

Ampere's law leads to the connection between the surface electric current distribution on the sphere and the spheroids in terms of the discontinuities in the tangential components of the magnetic induction fields:

$$\frac{4\pi}{c}\vec{K}\left(r{=}a, \vartheta, \varphi\right) {=} \hat{r} \times \left(\vec{B^e} {-} \vec{B^i}\right) = \left(B_0^e {-} B_0^i\right) \left[\frac{\hat{\varphi}}{h_\vartheta} \frac{dP_2^m\left(\cos\vartheta\right)}{d\vartheta} \begin{pmatrix} \cos\left(m\varphi\right) \\ \sin\left(m\varphi\right) \end{pmatrix} - \frac{\hat{\vartheta}}{h_\varphi} m P_2^m\left(\cos\vartheta\right) \begin{pmatrix} -\sin\left(m\varphi\right) \\ \cos\left(m\varphi\right) \end{pmatrix} \right], \quad (4.1)$$

$$\frac{4\pi}{c}\vec{K}\left(\xi = \xi_0, \vartheta, \varphi\right) = \hat{\xi} \times \left(\vec{B^e} - \vec{B^i}\right) = \left(B_0^e Q_2^m\left(\xi_0\right) - B_0^i P_2^m\left(\xi_0\right)\right) \left[\frac{\hat{\varphi}}{h_\vartheta} \frac{dP_2^m\left(\cos\vartheta\right)}{d\vartheta} \begin{pmatrix} \cos\left(m\varphi\right) \\ \sin\left(m\varphi\right) \end{pmatrix} - \frac{\hat{\vartheta}}{h_\varphi} m P_2^m\left(\cos\vartheta\right) \begin{pmatrix} -\sin\left(m\varphi\right) \\ \cos\left(m\varphi\right) \end{pmatrix} \right], \quad (4.2)$$

$$\frac{4\pi}{c}\vec{K}\left(\zeta = \zeta_0, \vartheta, \varphi\right) = \hat{\zeta} \times \left(\vec{B^e} - \vec{B^i}\right) = \left(B_0^e Q_2^m\left(i\zeta_0\right) - B_0^i P_2^m\left(i\zeta_0\right)\right) \left[\frac{\hat{\varphi}}{h_\vartheta} \frac{dP_2^m\left(\cos\vartheta\right)}{d\vartheta} \begin{pmatrix} \cos\left(m\varphi\right) \\ \sin\left(m\varphi\right) \end{pmatrix} - \frac{\hat{\vartheta}}{h_\varphi} m P_2^m\left(\cos\vartheta\right) \begin{pmatrix} -\sin\left(m\varphi\right) \\ \cos\left(m\varphi\right) \end{pmatrix} \right]. \quad (4.3)$$

The reader may notice the common formal ϑ and φ dependence of the linear current density $\vec{K}\left(\vartheta, \varphi\right)$ on the sphere and spheroids, taking into account the different scale factors and unit vectors involved, Eqs. (A.4-A.6). The factors in Eqs. (4.2) and (4.3) depending on the external and internal Legendre functions when combined with Eqs. (3.8) and (3.9) can be rewritten in terms of their respective Wronskians, Eqs. (A.25-A.26).

Next, we concentrate on the evaluation of the field lines for the ϑ and φ dependent linear current distributions of Eqs. (4.1)-(4.3), which depend only on the common angular factor.

For m=0, the lines are parallel circles with the distribution

$$\frac{\hat{\varphi}}{h_\vartheta} \frac{dP_2\left(\cos\vartheta\right)}{d\vartheta} h_\vartheta d\vartheta = 3\hat{\varphi} \sin\vartheta \cos\vartheta d\vartheta \quad (4.4)$$

eastward in the northern hemisphere and westward in the southern hemisphere, vanishing at the equator and also at the north and south poles, and with maximum intensities at ϑ=45° and $\vartheta = 135°$.

In general, the lines of the current distribution share the same direction of $\vec{K}$ at every point. Their differential form

$$d\vec{\ell} = \hat{e}_\vartheta h_\vartheta d\vartheta + \hat{e}_\varphi h_\varphi d\varphi \quad (4.5)$$

leads to the respective differential equations [13],

$$K_\varphi h_\vartheta d\vartheta = K_\vartheta h_\varphi d\varphi \quad (4.6)$$

for the distribution currents or coil windings in Eq. (4.1-4.3), for the other values of m.

For m=1, the $\hat{\varphi}$ and $\hat{\vartheta}$ components are respectively

$$\frac{1}{h_\vartheta} \frac{dP_2^1\left(\cos\vartheta\right)}{d\vartheta} \begin{pmatrix} \cos\varphi \\ \sin\varphi \end{pmatrix} h_\vartheta d\vartheta = 3 \times \left(\cos^2\vartheta - \sin^2\vartheta\right) \begin{pmatrix} \cos\varphi \\ \sin\varphi \end{pmatrix} d\vartheta, \quad (4.7)$$

$$-\frac{1}{h_\varphi}P_2^1(\cos\vartheta)\begin{pmatrix}-\sin\varphi\\ \cos\varphi\end{pmatrix}h_\varphi d\varphi=-3 \times\sin(\vartheta)\cos(\vartheta)\begin{pmatrix}-\sin\varphi\\ \cos\varphi\end{pmatrix}d\varphi, \quad (4.8)$$

leading to the lines via the respective differential equations

$$-\frac{\cos(2\vartheta)}{\sin(2\vartheta)}d\vartheta=-\frac{\sin\varphi}{\cos\varphi}d\varphi, \quad (4.9)$$

$$-2\frac{\cos(2\vartheta)}{\sin(2\vartheta)}d\vartheta=\frac{\cos\varphi}{\sin\varphi}d\varphi. \quad (4.10)$$

For a line passing through a point $\vartheta=\vartheta_0$, $\varphi=\varphi_0$ their respective solutions are:

$$\sin(2\vartheta)\cos\varphi=\sin(2\vartheta_0)\cos\varphi_0, \quad (4.11)$$

$$\sin(2\vartheta)\sin\varphi=\sin(2\vartheta_0)\sin\varphi_0. \quad (4.12)$$

These sets of lines have the same shape differing by 90° in longitudinal position. The currents vanish at the equator $\vartheta=90°$, and at meridians $\varphi=90°$ and 270°.

Similarly, for m=2 the $\hat{\varphi}$ and $\hat{\vartheta}$ components are

$$\frac{1}{h_\vartheta}\frac{dP_2^2(cos\vartheta)}{d\vartheta}\begin{pmatrix}\cos(2\varphi)\\ \sin(2\varphi)\end{pmatrix}h_\vartheta d\vartheta =6\sin\vartheta\cos\vartheta d\vartheta\begin{pmatrix}\cos(2\varphi)\\ \sin(2\varphi)\end{pmatrix}, \quad (4.13)$$

$$-\frac{1}{h_\varphi}P_2^2(\cos\vartheta)\;2\begin{pmatrix}-\sin(2\varphi)\\ \cos(2\varphi)\end{pmatrix}h_\varphi d\varphi =-3\sin^2\vartheta 2\begin{pmatrix}-\sin(2\varphi)\\ \cos(2\varphi)\end{pmatrix}d\varphi; \quad (4.14)$$

with the differential equations for the lines

$$\frac{\cos\vartheta}{\sin\vartheta}d\vartheta=-\frac{\sin(2\varphi)}{\cos(2\varphi)}d\varphi, \quad (4.15)$$

$$\frac{\cos\vartheta}{\sin\vartheta}d\vartheta=\frac{\cos(2\varphi)}{\sin(2\varphi)}d\varphi. \quad (4.16)$$

Their solutions for lines passing through $\vartheta=\vartheta_0$, $\varphi=\varphi_0$ are

$$\sin^2\vartheta\cos(2\varphi)=\sin^2\vartheta_0\cos(2\varphi_0), \quad (4.17)$$

$$\sin^2\vartheta\sin(2\varphi)=\sin^2\vartheta_0\sin(2\varphi_0). \quad (4.18)$$

These sets of lines also have the same shape differing by 45° in longitudinal positions. The currents vanish for $\varphi=45°$, 135°, 225° and 315° and φ=0°, 90°, 180° and 270°, respectively.

5. Graphic results and discussion

Figure 1 illustrates graphically the electric current distribution in windings on the surfaces of a pair of prolate spheroids, spheres and a pair of oblate spheroids, in the successive columns producing the constant gradient magnetic induction fields of Eqs. (1.1-1.5) in the successive rows. The readers may identify visually their characteristics, already described with words in the previous section. They may also recognize that the last pair for the sphere, also shares the same shapes with the previous pair, differing only in positions and orientations.

While the first configuration is the most familiar and simplest with rotational symmetry around the polar axis, the other four are its natural companions. The first one can be approximated with a pair of Maxwell coils [2], in analogy with the production of an almost uniform magnetic induction field with a pair of Helmholtz coils [13-15]. The authors are now examining the possibilities of approximating the other four configurations with the corresponding sets of four coils on spheres or spheroids, especially for their interest in the area of nuclear magnetic resonance imaging [2].

Since this is a teaching article, it is appropriate to include a few didactic observations and additional references on the physical problem and its methods of solution, which may be useful for upper level undergraduate and graduate courses of physics and engineering.

A. If the sources are known, the Biot-Savart's law is the natural tool to evaluate the magnetic induction field [2,9-10]. The same results may also be obtained using the alternative routes of the vector [6,8] or scalar [7] magnetic potential.

B. In the present manuscript, the aim is to find the possible sources of the target magnetic fields Eqs. (1.1-1.5). Section 4 illustrates how Ampere's law in its boundary condition form leads to the sources in Eqs. (4.1-4.3) and their respective components in Eqs. (4.4), (4.7-4.8), (4.13-4.14), and illustrated graphically in Fig. 1, for the respective spheroids and spheres.

C. The interested readers may compare the simplicity and harmonicity of the solution constructed in this article with those solutions reviewed in Ref. 2. Their difference resides in the pure quadrupolarity shared by fields and sources in the spherical and spheroidal geometries versus the pure quadrupolarity of the target field and the need of a large number of harmonic components in the other geometries.

D. Here we complement the bibliography of the spherical and spheroidal multipole harmonic functions, and of the imaging process itself.

i) Our didactic reference [12] has its illustrative counterparts in the later research literature: "Spherical Gradient Coil Research for Ultrafast Imaging" [16], restricted to the z-spherical gradient coil, equivalent of Eq. (4.4); and "Spherical Magnetic Moments System of Currents" [17], with the same contents as the first half of Sec. 3 in Ref. 12.

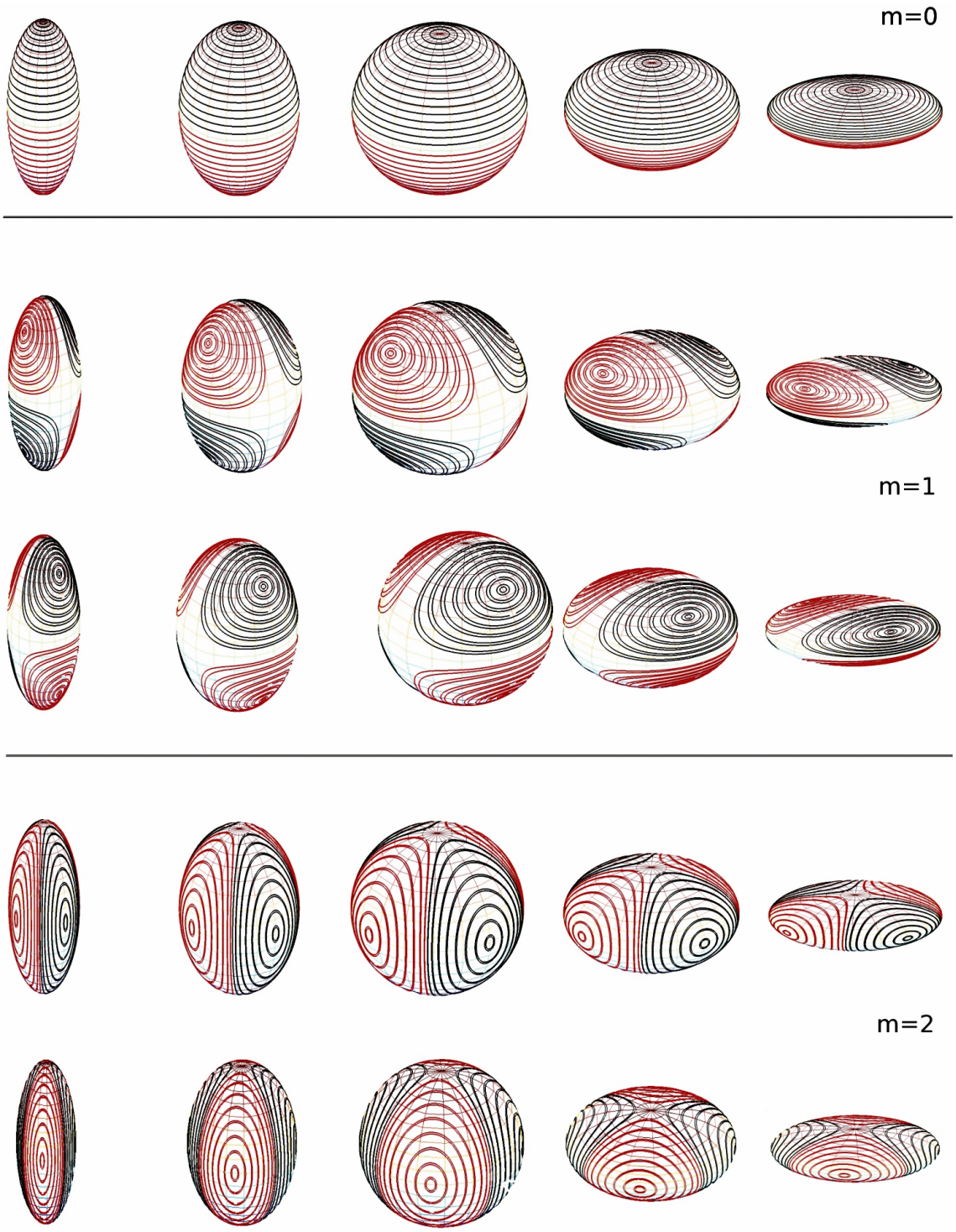

FIGURE 1. Surface current distrubutions or coil windings on a sequence of prolate spheroids, spheres and oblate spheroids in successive columns, and according to Eqs. (4.4), (4.11-4.12) and (4.17-4.18) in successive rows.

ii) Concerning the spheroidal geometries and others, our didactic articles "Harmonic Expansions of the Coulomb Potential in Cylindrical, Parabolic and Spheroidal Coordinates" [18] and "Complete Pure Dipole Spheroidal Electrostatic Fields and Sources" [19] have their research counterparts in "Using Prolate Spheroidal Magnetization Distributions for Magnetic Modeling" [20], "Separation of the Magnetic Fields into External and Internal Parts at the Surface of Prolate Spheroid" [21], "Application of Spheroidal Functions in Magnetostatics" [22], and "Gener-

ating Homogeneous Magnetostatic Field Inside Prolate and Oblate Ellipsoidal Coil" [23], respectively.

iii) We remind the reader about the limitation by choice of our work to the magnetostatics of the constant gradient magnetic fields and their spherical and spheroidal coil windings. References 1 and 2 illustrate the importance of such fields in the areas of neutral atom traps and magnetic resonance imaging. The interested readers are invited to read the respective Nobel Prize lectures cited in the second paragraph in order to appreciate the advances in both areas. For the readers with specific interests in the imaging process itself we add the illustrative references "Fast Spheroidal Multipole Imaging of Elementary Magnetic Sources on the Axis" [24] and "Perturbative Analytical Solutions of the Magnetic Forward Problem for Realistic Volume Conductors" [25].

E. The Appendix is included in order to make the article self-contained. Its reading allows understanding the geometry of the respective coordinates and their connections, the structure of their scale factors and unit vectors, which determine the structure of the Laplace operators, as well as the separability and integrability of the Laplace equations, leading to the well-behaved spheroidal harmonic functions inside and outside the respective spheroids.

F. For the readers who feel more confortable using the magnetic vector potential, it is straightforward to construct it as the counterparts replacing Eqs. (1.6-1.10), with the corresponding modifications in Secs. 2 and 3. The treatment of Sec. 4 remains the same.

Appendix

Prolate and oblate spheroidal coordinates and spheroidal harmonic functions

This Appendix starts from the transformation equations from spheroidal to Cartesian coordinates, to obtain their inverses, the scale factors and unit vectors, the Laplace operators, and the solutions of the Laplace equation needed in the main body of the article [26-28].

1. Transformation equations:

$$\begin{aligned} x &= f\sqrt{\xi^2-1}\sin\vartheta\cos\varphi = f\sqrt{\zeta^2+1}\sin\vartheta\cos\varphi \\ y &= f\sqrt{\xi^2-1}\sin\vartheta\sin\varphi = f\sqrt{\zeta^2+1}\sin\vartheta\sin\varphi \\ z &= f\xi\cos\vartheta = f\zeta\cos\vartheta \end{aligned} \tag{A.1}$$

2. The inverse transformations

$$\begin{aligned} \frac{x^2+y^2}{f^2\left(\xi^2-1\right)}+\frac{z^2}{f^2\xi^2} &= 1 = \frac{x^2+y^2}{f^2\left(\zeta^2+1\right)}+\frac{z^2}{f^2\zeta^2} \\ \frac{z^2}{f^2\cos^2\vartheta}-\frac{x^2+y^2}{f^2\sin^2\vartheta} &= 1 = \frac{x^2+y^2}{f^2\sin^2\vartheta}-\frac{z^2}{f^2\cos^2\vartheta} \\ \varphi &= \tan^{-1}\frac{y}{x} \end{aligned} \tag{A.2}$$

allow to identify prolate spheroids with focii at $(x=0, y=0, z=\pm f)$ for fixed values of $\xi \in [1,\infty)$ and eccentricity $1/\xi$, confocal two-sheet hyperboloids with real axis along the *z*-axis for fixed values of $\vartheta \in [0,\pi]$ and eccentricity $1/\cos\vartheta$; confocal oblate spheroids with focii at $(x=f\cos\varphi,\ y=f\sin\varphi,\ z=0)$ for fixed values of $\zeta \in [0,\infty)$ and eccentricity $1/\sqrt{\zeta^2+1}$, confocal one-sheet hyperboloids with real axis along the *xy* plane for fixed values of $\vartheta \in [0,\pi]$ and eccentricity $1/\sin\vartheta$; common meridian half planes with a common edge at thez-axis for fixed values of $\varphi \in [0,2\pi]$. Both sets of coordinates become spherical coordinates in the respective limits: $\xi\to\infty,\ f\to 0,\ f\xi\to r$; $\zeta\to\infty,\ f\to 0,\ f\zeta\to r$. The respective hyperboloids become circular cones.

3. The scale factors and unit vectors follow from the evaluation of the displacement vector,

$$\begin{aligned} d\vec{r} &= \hat{i}dx+\hat{j}dy+\hat{k}dz \\ &= f\left[\left(\hat{i}\cos\varphi+\hat{j}\sin\varphi\right)\frac{\xi}{\sqrt{\xi^2-1}}\sin\vartheta+\hat{k}\cos\vartheta\right]d\xi \\ &+ f\left[\sqrt{\xi^2-1}\cos\vartheta\left(\hat{i}\cos\varphi+\hat{j}\sin\varphi\right)-\hat{k}\xi\sin\vartheta\right]d\vartheta \\ &+ f\sqrt{\xi^2-1}\sin\vartheta\left(-\hat{i}\sin\varphi+\hat{j}\cos\varphi\right)d\varphi \\ &= f\left[\left(\hat{i}\cos\varphi+\hat{j}\sin\varphi\right)\frac{\zeta}{\sqrt{\zeta^2+1}}\sin\vartheta+\hat{k}\cos\vartheta\right]d\zeta \\ &+ f\left[\sqrt{\zeta^2+1}\cos\vartheta\left(\hat{i}\cos\varphi+\hat{j}\sin\varphi\right)-\hat{k}\zeta\sin\vartheta\right]d\vartheta \\ &+ f\sqrt{\zeta^2+1}\sin\vartheta\left(-\hat{i}\sin\varphi+\hat{j}\cos\varphi\right)d\varphi \\ &= \hat{\xi}h_\xi d\xi+\hat{\vartheta}h_\vartheta d\vartheta+\hat{\varphi}h_\varphi d\varphi \\ &= \hat{\zeta}h_\zeta d\zeta+\hat{\vartheta}h_\vartheta d\vartheta+\hat{\varphi}h_\varphi d\varphi \end{aligned} \tag{A.3}$$

Consequently,

$$\begin{aligned} h_\xi &= f\sqrt{\frac{\xi^2-\cos^2\vartheta}{\xi^2-1}}, \qquad h_\vartheta = f\sqrt{\xi^2-\cos^2\vartheta}, \\ h_\varphi &= f\sqrt{\xi^2-1}\sin\vartheta, \end{aligned} \tag{A.4}$$

$$h_\zeta = f\sqrt{\frac{\zeta^2+\cos^2\vartheta}{\zeta^2+1}}, \qquad h_\vartheta = f\sqrt{\zeta^2+\cos^2\vartheta},$$

$$h_\varphi = f\sqrt{\zeta^2+1}\sin\vartheta, \tag{A.5}$$

$$\hat{\xi} = \frac{\xi\sin\vartheta\left(\hat{i}\cos\varphi+\hat{j}\sin\varphi\right)+\hat{k}\sqrt{\xi^2-1}\cos\vartheta}{\sqrt{\xi^2-\cos^2\vartheta}},$$

$$\hat{\vartheta} = \frac{\sqrt{\xi^2-1}\cos\vartheta\left(\hat{i}\cos\varphi+\hat{j}\sin\varphi\right)-\hat{k}\xi\sin\vartheta}{\sqrt{\xi^2-\cos^2\vartheta}},$$

$$\hat{\varphi} = \left(-\hat{i}\sin\varphi+\hat{j}\cos\varphi\right),$$

$$\hat{\zeta} = \frac{\zeta\sin\vartheta\left(\hat{i}\cos\varphi+\hat{j}\sin\varphi\right)+\hat{k}\sqrt{\zeta^2+1}\cos\vartheta}{\sqrt{\zeta^2+\cos^2\vartheta}},$$

$$\hat{\vartheta} = \frac{\sqrt{\zeta^2+1}\cos\vartheta\left(\hat{i}\cos\varphi+\hat{j}\sin\varphi\right)-\hat{k}\zeta\sin\vartheta}{\sqrt{\zeta^2+\cos^2\vartheta}}. \tag{A.6}$$

Each set of unit vectors $\left(\hat{\xi},\hat{\vartheta},\hat{\varphi}\right)$ and $\left(\hat{\zeta},\hat{\vartheta},\hat{\varphi}\right)$ is an orthonormal right-handed triad.

4. The Laplace operator becomes

$$\nabla^2 = \frac{1}{f^2\left(\xi^2-\cos^2\vartheta\right)} \times\left[\frac{\partial}{\partial\xi}\left(\xi^2-1\right)\frac{\partial}{\partial\xi}+\frac{1}{\sin\vartheta}\frac{\partial}{\partial\vartheta}\sin\vartheta\frac{\partial}{\partial\vartheta}\right] + \frac{1}{f^2\left(\xi^2-1\right)\sin^2\vartheta}\frac{\partial^2}{\partial\varphi^2},$$

$$\nabla^2 = \frac{1}{f^2\left(\zeta^2+\cos^2\vartheta\right)} \times\left[\frac{\partial}{\partial\zeta}\left(\zeta^2+1\right)\frac{\partial}{\partial\zeta}+\frac{1}{\sin\vartheta}\frac{\partial}{\partial\vartheta}\sin\vartheta\frac{\partial}{\partial\vartheta}\right] + \frac{1}{f^2\left(\zeta^2+1\right)\sin^2\vartheta}\frac{\partial^2}{\partial\varphi^2}. \tag{A.7}$$

5. The Laplace equation takes the respective forms

$$\left\{\frac{1}{f^2\left(\xi^2-\cos^2\vartheta\right)}\left[\frac{\partial}{\partial\xi}\left(\xi^2-1\right)\frac{\partial}{\partial\xi}+\frac{1}{\sin\vartheta}\frac{\partial}{\partial\vartheta}\sin\vartheta\frac{\partial}{\partial\vartheta}\right] + \frac{1}{f^2\left(\xi^2-1\right)\sin^2\vartheta}\frac{\partial^2}{\partial\varphi^2}\right\}\phi\left(\xi,\vartheta,\varphi\right)=0,$$

$$\left\{\frac{1}{f^2\left(\zeta^2+\cos^2\vartheta\right)}\left[\frac{\partial}{\partial\zeta}\left(\zeta^2+1\right)\frac{\partial}{\partial\zeta}+\frac{1}{\sin\vartheta}\frac{\partial}{\partial\vartheta}\sin\vartheta\frac{\partial}{\partial\vartheta}\right] + \frac{1}{f^2\left(\zeta^2+1\right)\sin^2\vartheta}\frac{\partial^2}{\partial\varphi^2}\right\}\phi\left(\zeta,\vartheta,\varphi\right)=0. \tag{A.8}$$

6. Solution of the Laplace equations. Both equations admit factorizable solutions

$$\phi\left(\xi,\vartheta,\varphi\right) = \Xi\left(\xi\right)\Theta\left(\vartheta\right)\Phi\left(\varphi\right), \tag{A.9}$$

$$\phi\left(\zeta,\vartheta,\varphi\right) = Z\left(\zeta\right)\Theta\left(\vartheta\right)\Phi\left(\varphi\right). \tag{A.10}$$

The common angular factors satisfy the same differential ordinary equations as those in spherical coordinates

$$\frac{d^2\Phi\left(\varphi\right)}{d\varphi^2} = -m^2\Phi\left(\varphi\right), \tag{A.11}$$

$$\left[\frac{1}{\sin\vartheta}\frac{d}{d\vartheta}\sin\vartheta\frac{d}{d\vartheta}-\frac{m^2}{\sin^2\vartheta}\right]\Theta\left(\vartheta\right) = -\ell\left(\ell+1\right)\Theta\left(\vartheta\right), \tag{A.12}$$

satisfying the same boundary conditions with the respective integer eigenvalues $m=1,2,\ldots,\ell$ and $\ell=0,1,2,\ldots$

The respective spheroidal coordinate ordinary differential equations become

$$\left[\frac{d}{d\xi}\left(\xi^2-1\right)\frac{d}{d\xi}-\frac{m^2}{\xi^2-1}\right]\Xi\left(\xi\right)=\ell\left(\ell+1\right)\Xi\left(\xi\right), \tag{A.13}$$

$$\left[\frac{d}{d\zeta}\left(\zeta^2+1\right)\frac{d}{d\zeta}+\frac{m^2}{\zeta^2+1}\right]Z\left(\zeta\right)=\ell\left(\ell+1\right)Z\left(\zeta\right), \tag{A.14}$$

involving the same separation constants with appropriate signs.

The linearly independent solutions in φ are chosen to have well-definded parities

$$\Phi_m\left(\varphi\right) = \begin{pmatrix}\cos\left(m\varphi\right)\\ \sin\left(m\varphi\right)\end{pmatrix}, \tag{A.15}$$

while those in ϑ are identified as associated Legendre polynomials,

$$P_\ell^m\left(\cos\vartheta\right) = \sin^m\vartheta\frac{d^m}{d\left(\cos\vartheta\right)^m}P_\ell\left(\cos\vartheta\right). \tag{A.16}$$

Let us recall that Eq. (A.12) can be rewritten, after the change of variable $\eta=\cos\vartheta$, in the form

$$\left[\frac{d}{d\eta}\left(1-\eta^2\right)\frac{d}{d\eta}-\frac{m^2}{1-\eta^2}\right]P_\ell^m\left(\eta\right) = -\ell\left(\ell+1\right)P_\ell^m\left(\eta\right) \tag{A.17}$$

The reader may recognize that Eq. (A.13) is the same as the last one for the interval $1<\xi<\infty$. Its solutions are therefore associated Legendre polynomials $P_\ell^m\left(\xi\right)$ or associated Legendre functions of the second kind $Q_\ell^m\left(\xi\right)$. In turn, after the change of variables $\eta\to i\zeta$ or $\xi\to i\zeta$, Eq. (A.17) or (A.13) become Eq. (A.14). Consequently, the latter admits solutions $P_\ell^m\left(i\zeta\right)$ and $Q_\ell^m\left(i\zeta\right)$. The connection between the prolate and oblate spheroidal harmonic functions is via the analytic continuation $\xi\to i\zeta$.

In particular the quadrupole ℓ=2 harmonic functions of our interest are:

$$P_2(\xi)P_2(\cos\vartheta) = \frac{3\xi^2-1}{2}\frac{3\cos^2\vartheta-1}{2}, \tag{A.18}$$

$$P_2^1(\xi)P_2^1(\cos\vartheta)\begin{pmatrix}\cos\varphi\\ \sin\varphi\end{pmatrix} = 3\xi\sqrt{\xi^2-1}\;3\sin\vartheta\cos\vartheta\begin{pmatrix}\cos\varphi\\ \sin\varphi\end{pmatrix}, \tag{A.19}$$

$$P_2^2(\xi)P_2^1(\cos\vartheta)\begin{pmatrix}\cos\varphi\\ \sin\varphi\end{pmatrix} = 3\left(\xi^2-1\right)\;3\sin^2\vartheta\begin{pmatrix}\cos(2\varphi)\\ \sin(2\varphi)\end{pmatrix}, \tag{A.20}$$

in the interior of prolate spheroids, with the replacements

$$P_2(i\zeta) = \frac{3\zeta^2+1}{2}, \tag{A.21}$$

$$P_2^1(i\zeta) = 3\zeta\sqrt{\zeta^2+1}, \tag{A.22}$$

$$P_2^2(i\zeta) = 3\left(\zeta^2+1\right), \tag{A.23}$$

in the interior of oblate spheroids.

The respective harmonic functions for the outside involve the Legendre functions:

$$Q_2(\xi) = \frac{1}{2}P_2(\xi)\,ln\left(\frac{\xi+1}{\xi-1}\right) - \frac{3\xi}{2},$$

$$Q_2^m(\xi) = \left(\xi^2-1\right)^{\frac{m}{2}}\frac{d^mQ_2(\xi)}{d\xi^m}, \tag{A.24}$$

for $m = 0, 1, 2$, respectively, for the prolate spheroids; and their counterparts with $\xi \to i\zeta$, $\xi^2-1 \to \zeta^2+1$ for the oblate spheroids.

The linear independence of the Legendre polynomials and Legendre function of the second kind is expressed by their Wronskians:

$$P_\ell^m(\xi)\frac{dQ_\ell^m(\xi)}{d\xi} - \frac{dP_\ell^m(\xi)}{d\xi}Q_\ell^m(\xi) = -\frac{1}{\xi^2-1}, \tag{A.26}$$

$$P_\ell^m(i\zeta)\frac{dQ_\ell^m(i\zeta)}{d(i\zeta)} - \frac{dP_\ell^m(i\zeta)}{d(i\zeta)}Q_\ell^m(i\zeta) = \frac{1}{\zeta^2+1}. \tag{A.27}$$

1. V. Gomer *et al.*, *Hyperfine Interactions* **109** (1997) 281.
2. S.S. Hidalgo-Tobon, *Concepts in Magnetic Resonance* **36A** (2010) 223.
3. http://nobelprize.org/nobel_prizes/physics/laureates/1997/
4. http://nobelprize.org/nobel_prizes/physics/laureates/2001/
5. http://nobelprize.org/nobel_prizes/medicine/laureates/2003/
6. H. Sanchez Lopez, F. Liu, M. Poole, and S. Crozier, *IEEE Trans. on Magnetics* **45** (2009) 767.
7. D. Green, J. Leggett, and R. Bowtell, *Magnetic Resonance in Medicine* **54** (2005) 656.
8. M. Poole and R. Bowtell, *Concepts in Magnetic Resonance* **31B** (2007) 162.
9. V. Vech, H. Zhao, G.J. Galloway, D. M. Doddrell, and I.M. Brereton, *Concepts in Magnetic Resonance* **27B** (2005) 17.
10. V. Vech, H. Zhao, D.M. Doddrell, and I.M. Brereton, G.J. Galloway, *Concepts in Magnetic Resonance* **27B** (2005) 25.
11. C.H. Moon, H.W. Park, M.H. Cho, and S.Y. Lee, *Meas. Sci. Technol.* **11** (2000) N89.
12. E. Ley-Koo and A. Góngora-T. *Rev. Mex. Fís* **34** (1988) 645.
13. J.R. Reitz, F.J. Milford, and R.W. Christy, *Foundations of Electromagnetic Theory* (Addison-Wesley, Reading Mass 1979).
14. M.A. Heald, and J.B. Marion, *Classical Electromagnetic Radiation* 3th Ed., (Saunders College Publishing, USA 1995).
15. J.D. Jackson, *Classical Electrodynamics* 2nd. Ed., (Wiley, New York 1975).
16. H. Liu, L.S. Petropoulos, *J. Appl Phys* **81** (1997) 3853.
17. V.P. Kazantsev, *Russian Physics J.* **42** (1999) 916.
18. E. Ley-Koo , A. Góngora T. *Rev. Mex. Fís*. **39** (1993) 785.
19. E. Ley-Koo, *Rev. Mex. Fís. E* **55** (2009) 1.
20. D.A. Nixon and F.E. Baker, *J. Appl. Phys.* **52** (1981) 539.
21. V.P. Golovkov and T.I. Zvereva, *Geomagnetism and Aeronomy* **34** (1995) 851.
22. A.V. Kilidishev, *IEEE Trans. on Magnetics* **40** (2004) 846.
23. D.U. Zivaljevic and S.R. Aleksic, *Int J. Electron. Commun. (AEU)* **61** (2007) 637.
24. G. Nolte, T. Fieseler, and G. Curio, *J. Appl Phys* **89** (2001) 2360.
25. A.V. Kildishev and J.A. Nyenhuis, *J. Appl Phys* **89** (2001) 6716.
26. E.W. Hobson, *The Theory of Spherical and Ellipsoidal Harmonics* (Cambridge University Press 1931).
27. J. Arfken, *Mathematical Methods of Physics* (Academic Press, USA 1966).
28. M. Abramowitz and I. Stegun, *Handbook of Mathematical Functions with Formulas, Graphs, and Mathematical Tables* (Dover Publications 1972).